Dyes and Pigments 92 (2012) 1062–1068

Contents lists available at ScienceDirect

Dyes and Pigments

journal homepage: www.elsevier.com/locate/dyepig

Synthesis and applications of 3,6-carbazole-based conjugated side-chain copolymers containing complexes of 1,10-phenanthroline with Zn(II), Cd(II) and Ni(II) for dye-sensitized solar cells

Lihui Guo, Jinyan Deng, Lirong Zhang, Qian Xiu, Gaojun Wen, Chaofan Zhong*

Key Laboratory of Environmentally Friendly Chemistry and Applications of Ministry of Education, Xiangtan University, College of Chemistry, Xiangtan, Hunan 411105, PR China

ARTICLE INFO

Article history:
Received 22 April 2011
Received in revised form
13 July 2011
Accepted 15 July 2011
Available online 26 July 2011

Keywords:
Dye-sensitized solar cells
Polymeric metal complexes
1,10-Phenanthroline
Polycarbazole
Photovoltaic performance
π-conjugated copolymers

ABSTRACT

Three novel donor-acceptor polymeric metal complexes based on polycarbazole containing complexes of 1,10-phenanthroline with Zn(II), Cd(II) and Ni(II) have been synthesized by the Ullmann reaction and characterized by gel permeation chromatography, FT-IR, UV–visible absorption and photoluminescence spectroscopy, cyclic voltammetry and elemental analysis. The application of these organometallic polymers in fabricated dye-sensitized solar cells has been studied. The solar cells exhibited good device performance with a power conversion efficiency of up to 0.44%, under simulated air mass 1.5 G solar irradiation.

1. Introduction

The generation of energy is one of the most important scientific and technological challenges in the 21st century. Harvesting energy directly from sunlight using photovoltaic cells is a very important way to address growing global energy needs with a renewable resource. Dye-sensitized solar cells (DSSCs) based on mesoporous nanocrystalline TiO_2 films have attracted significant attention due to their relatively low cost and high sunlight-to-electric power conversion efficiencies of 11–12.5% [1–5].

In recent years, many conjugated polymers have been developed and used as dye sensitizers for DSSCs [6–12]. Organic dyes as an alternative to the Ru complex sensitizers exhibit many advantages, such as diversity of molecular structures, high molar extinction coefficient, simple synthesis as well as low cost and relatively low environmental issues. Conjugated polymers having D–A architectures have been extensively studied by using fused heterocyclic electron rich segments, such as carbazole [13,14], diketopyrrolopyrrole [15], indoline [16], dithienopyrrole [17], dithienosilole [18], fluorene [19,20], and phenothiazine [21,22] as electron donating building blocks for DSSCs. Carbazole is a well-known electroluminescent and hole-transporting unit [23] and can be easily functionalized on the 3,6- [24], 2,7- [25], or N-positions [26]. Carbazole has emerged as a promising electron-donating moiety for the construction of D–A polymers due to its excellent thermal and photochemical stability, relatively high hole mobility and good solubility in common organic solvents. For example, Ko and co-workers developed some organic dyes containing an *N*-aryl carbazole moiety for DSSCs, the JK-25 (Scheme 1) sensitized cell gave an overall conversion efficiency of 5.15%, under AM 1.5 G. Under the same test conditions, a DSSCs based on N719 (Scheme 1) showed 7.8% efficiency [27].

As an important ligand, 1,10-phenanthroline has been extensively used in functional metal complexes. The unit is rigid, and provides two aromatic nitrogens whose unshared electron pairs are beautifully placed to act cooperatively in binding transition metal cations. Considering the unique combination of morphology, chemical stabilities, redox properties, photophysical properties and excited state lifetime, some researchers have used metal-phenanthroline complexes in DSSCs. It has been shown that Cu(I) complexes with 2,9-disubstituted 1,10-phenanthroline ligands possessed similar photophysical properties to archetypal $[Ru(bpy)_3]^{2+}$ salts (bpy = 2,2′-bipyridine) [28–31].

* Corresponding author. Tel.: +86 731 58292202; fax: +86 731 52380072.
E-mail address: zhongcf798@yahoo.com.cn (C. Zhong).

0143-7208/$ – see front matter © 2011 Elsevier Ltd. All rights reserved.
doi:10.1016/j.dyepig.2011.07.007

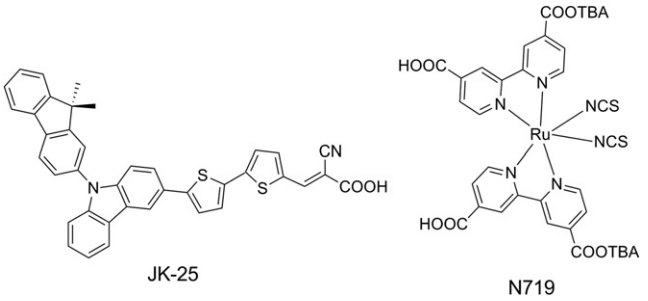

Scheme 1. Structure of JK-25 and N719.

In this paper a series of D–A complexes containing carbazole as the electron donor and metal-phenanthroline as the electron acceptor were synthesized. The π-conjugated copolymers are tuned by metal complexes in the branched chain in order to change the photophysical and electrochemical properties and thus improve the photovoltaic performance. The optical, thermal and photovoltaic properties of the resulting polymers were investigated.

2. Experimental method

2.1. Materials

$NiCl_2(PPh_3)_2$, Carbazole, 1,10-phenanthroline and NBS were obtained from Aldrich Chemical Co. and used as received. N,N-Dimethylformamide was dried by distillation over CaH_2, ethanol was dried over molecular sieves and freshly distilled prior to use. All chemicals used were of an analytical grade. Solvents were purified with conventional methods.

2.2. Instrument and measurements

All ^1H NMR spectra were performed in $CDCl_3$ and recorded on a Bruker NMR 400 spectrometer, and using TMS (0.00 ppm) as the internal reference. Infrared (FT-IR) spectra were recorded on KBr pellets (250 mg of dried KBr and 2 mg of lyophilized samples) with a Perkin–Elmer Spectrum One Fourier transform infrared spectrophotometer over the 4000–450 cm^{-1} range, at a rate of 16 nm/s. Thermogravimetric analyses were run on a Shimadzu TGA-7 instrument under a nitrogen atmosphere at a heating rate of 20 K/min from 25 °C to 900 °C. Differential Scanning Calorimetry was performed on materials using a Perkin–Elmer DSC-7 thermal analyzer under a nitrogen atmosphere at a heating rate of 20 °C/min from 25 °C to 900 °C. UV–Vis spectra were taken on a Lambda 25 spectro- photometer. Samples were dissolved in DMF and diluted to a concentration (10^{-4}–10^{-5} M). Photoluminescent spectra were taken on a Perkin–Elmer LS55 luminescence spectrometer with a xenon lamp as the light source. Elemental analysis for C, H and N was carried out using a Perkin–Elmer 2400 II instrument; metal ion and chlorine ion were measured by chemical method. Gel permeation chromatography (GPC) analyses were performed using a Water 2414 system equipped with a set of HT3, HT4 and HT5, L-styrayel columns with DMF as an eluent (1.0 ml/min) at 80 °C, calibrated with a polystyrene standard. Cyclic voltammetry was conducted on a CH Instruments chi630c Electrochemical Workstation, in a 0.1 mol/L$[Bu_4N]BF_4$ DMF solution at a scan rate of 100 mV/s at room temperature. The working electrode was a glassy carbon electrode, the auxiliary electrode was a Pt wire electrode, and a saturated calomel electrode (SCE) was used as reference electrode.

2.3. General procedures for fabrication of the DSSCs devices

Titania paste was prepared following a procedure: Fluorine-doped SnO_2 conducting glass (FTO) were cleaned and immersed in aqueous 40 mM $TiCl_4$ solution at 70 °C for 30 min, then washed with water and ethanol, sintered at 450 °C for 30 min. The 20–30 nm particles sized TiO_2 colloid was coated onto the above FTO glass by the sliding glass rod method to obtain a TiO_2 film of 10–15 μm thickness. After drying, the TiO_2-coated FTO glass were sintered at 450 °C for 30 min, then treated with $TiCl_4$ solution and calcined at 450 °C for 30 min again. After cooling to 100 °C, the TiO_2 electrodes were soaked in 0.5 mmol/L dye samples in dimethyl sulfoxide (DMSO) solution, and then kept at room temperature in the dark for 24 h. A 3-methoxypropionitrile solution containing LiI (0.5 mol/L), I_2 (0.05 mol/L), and 4-tert-butylpyridine (TBP) (0.5 mol/L) was used as the electrolyte. Pt foil was used as the counter electrode and was clipped onto the TiO_2 used as the working electrode. The photoelectrochemical performance of the solar cell was measured using a Keithley 2602 Source meter controlled by a computer. The cell parameters were obtained under an incident light with intensity 100 mW/cm^2, which was generated by a 150 W Xe lamp passing through an AM 1.5 G filter.

2.4. Synthesis

2.4.1. Synthesis of ***NPC***

Carbazole (1.67 g, 10 mmol), K_2CO_3 (1.50 g, 10 mmol), CuI (0.32 g, 2 mmol) and 3-bromo-1,10-phenanthroline (synthesized according to the literature [32]) (2.77 g, 10 mmol) were dissolved in nitrobenzene (20 mL) under nitrogen. Then the mixture was stirring at 200 °C for 24 h. The reaction system was then allowed to cool to room temperature and the volume of solvent was reduced pressure distillation to ca. 30% of its original size. The crude product was purified by column chromatography on an aminopropylated silica gel and recrystallization from chloroform/methanol to give 1.45 g yellow solid (yield 40%). ^1H NMR ($CDCl_3$, δ, ppm): 9.54 (s, 1H), 8.57 (s, 1H), 8.24 ~ 8.22 (d, 2H), 8.03 (s, 1H), 7.58 ~ 7.56 (d, 2H), 7.52 ~ 7.48 (t, 3H), 7.42 ~ 7. 38 (t, 3H), 7.27 (d, 2H). FT-IR (KBr, cm^{-1}): 1608 (C=N), 1494 (C=C), 1224, 1163 (C–N), 744, 720; For $[C_{24}H_{15}N_3]$: C, 83.46; H, 4.38; N, 12.16; Found: C, 83.54; H, 4.25; N, 12.21%.

2.4.2. Synthesis of ***DBPC***

A modified version of a previously reported method [33] was used. **NPC** (0.36 g, 1 mmol) was dissolved in DMF (20 mL) at 0 °C with stirring. To this was dropped a solution of NBS (0.36 g, 2 mmol) in DMF (10 mL). After being stirred at room temperature for 2 h, the solution was poured into water (500 mL), filtered, and washed with water (500 mL). The yellow residue was recrystallized in ethanol and gave yellow solid (0.44 g, 85%). ^1H NMR ($CDCl_3$, δ, ppm): 9.50 ~ 9.47 (d, 1H), 8.56 ~ 8.53 (d, 1H), 8.35 ~ 8.30 (d, 2H), 8.20 ~ 8.17 (d, 1H), 8.05 (s, 1H), 7.63 ~ 7.52 (dd, 4H), 7.44 ~ 7.40 (t, 3H). FT-IR (KBr, cm^{-1}): 1607 (C=N), 1468 (C=C), 1224, 1162 (C–N), 801, 735 (1,10-phen or carbazole C–H), 577 (C–Br). Anal. Calcd. For $[C_{24}H_{13}N_3Br_2]$: C, 57.29; H, 2.60; N, 8.35; Found: C, 57.11; H, 2.52; N, 8.13%.

2.4.3. Synthesis of ***DBPC-Zn-p***

An ethanol solution (10 mL) of $Zn(CH_3COO)_2{\cdot}2H_2O$ (0.11 g, 0.5 mmol) was dropped to a mixed THF solution (20 mL) of **DBPC** (0.252 g, 0.5 mmol) and 1,10-phenanthroline (0.099 g, 0.5 mmol). The reaction mixture was neutralized carefully with 1 M aq sodium hydroxide until neutral to slightly acidic pH and was heated under reflux overnight. The collected product was recrystallized from ethanol. Filtered, washed with ethanol and water repeatedly, the

yellow precipitate was collected (0.36 g, yield 83%). FT-IR (KBr, cm^{-1}): 1606 (C═N), 1478 (C═C), 1107 (C═N–M). Anal. Calcd. For [$C_{40}H_{27}O_4N_5Br_2Zn$]: C, 55.42; H, 3.14; N, 8.07; Found: C, 55.53; H, 3.21; N, 8.02%.

*2.4.4. Synthesis of **DBPC-Cd-p***

In the same manner as described for **DBPC-Zn-p**. Yield 86%, a yellow solid. FT-IR (KBr, cm^{-1}): 1592 (C═N), 1473 (C═C), 1106 (C═N–M). Anal. Calcd. For [$C_{36}H_{21}N_5Br_2Cl_2Cd$]: C, 49.89; H, 2.44; N, 8.08; Found: C, 49.92; H, 2.51; N, 8.14%.

*2.4.5. Synthesis of **DBPC-Ni-p***

In the same manner as described for **DBPC-Zn-p**. Yield 78%, a yellow solid. FT-IR (KBr, cm^{-1}): 1590 (C═N), 1475 (C═C), 1103 (C═N–M). Anal. Calcd. For [$C_{36}H_{21}N_7Br_2O_6Ni$]: C, 49.92; H, 2.44; N, 11.32; Found: C, 50.12; H, 2.61; N, 11.14%.

*2.4.6. Synthesis of copolymer **P1***

The copolymer was synthesized by the Yamamoto coupling method according to the literature [34]. **DBPC-Zn-p** (0.347 g, 0.4 mmol), bis(triphenylphosphine) nickel(II) chloride (0.26 g, 0.4 mmol), 3,6-dibromo-9-N-octyl carbazole (synthesized according to the literature [35]) (0.175 g, 0.4 mmol), zinc (0.13 g, 2 mmol), triphenylphosphine (0.209 g, 0.8 mmol) and a little bipyridine (0.006 g, 0.038 mmol) were dissolved in DMF (15 mL) under nitrogen. Then the mixture was stirring at 90 °C for 36 h. A yellow solid was precipitated into a large excess of methanol solution. The crude product was washed with methanol, distilled water and THF sequentially, and then dried in vacuum at 60 °C for one day to afford a pale yellow solid (0.25 g, 49%). FT-IR (KBr, cm^{-1}): 1584 (C═N), 1508 (C═C), 1105 (C═N–M). Anal. Calcd. For [$C_{60}H_{56}O_4N_6Zn$]: C, 72.75; H, 5.70; N, 8.48; Found: C, 72.83; H, 5.72; N, 8.43%. Mn = 5.0 K, Mw/Mn = 1.81.

*2.4.7. Synthesis of copolymer **P2***

With the similar synthetic method as copolymer **P1** afford a yellow solid (0.27 g, 50%). FT-IR (KBr, cm^{-1}): 1591 (C═N), 1504 (C═C), 1049 (C═N–M). Anal. Calcd. For [$C_{56}H_{44}N_6Cl_2Cd$]: C, 68.33; H, 4.51; N, 8. 54; Found: C, 68.48; H, 4.59; N, 8.49%. Mn = 4.6 K, Mw/Mn = 1.67.

*2.4.8. Synthesis of copolymer **P3***

With the similar synthetic method as copolymer **P1** afford a yellow solid (0.27 g, 45%). FT-IR (KBr, cm^{-1}): 1591 (C═N), 1504 (C═C), 1049 (C═N–M). Anal. Calcd. For [$C_{56}H_{44}O_6N_8$ Ni]: C, 68.37; H, 4.51; N, 11.39; Found: C, 68.18; H, 4.58; N, 11.47%. Mn = 5.4 K, Mw/Mn = 1.47.

3. Results and discussion

3.1. Synthesis and characterization

Scheme 2 outlines the synthetic routes to the ligand **DBPC** which was synthesized by the Ullmann reaction [36] and three

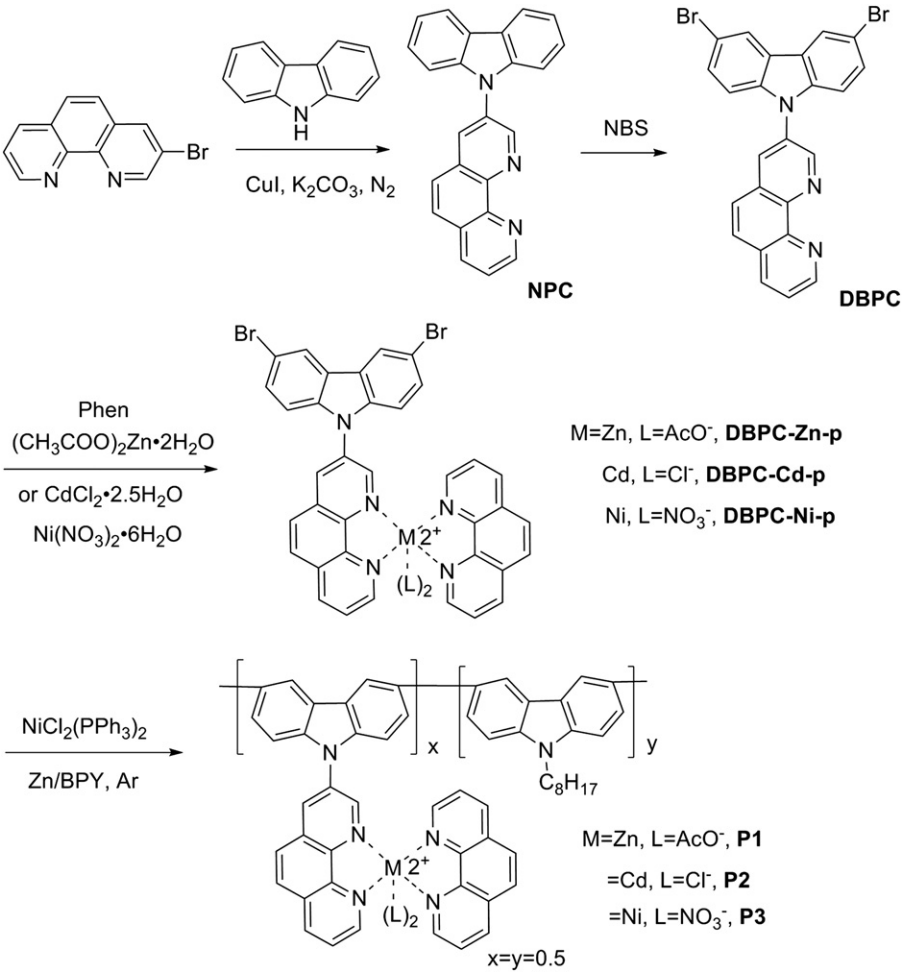

Scheme 2. Synthesis of the comonomers and copolymers **P1**–**P3**.

polymers **P1**–**P3** which were synthesized by a Yamamoto coupling protocol [37].

Fig. 1 displays the ^{1}H NMR spectrum of **DBPC**. The signals for the protons ortho to the N atoms in 1,10-phenanthroline are observed at 9.50 ppm and 8.56 ppm. Signals between 7.4 and 8.5 ppm are attributed to the remaining protons of 1,10-phenanthroline and carbazole moieties.

The IR spectra of the ligand **DBPC** and the copolymers **P1**–**P3** show a sharp absorption peak at 1608 cm^{-1} which is ascribed to the C═N stretching of 1,10-phenanthroline unit. Absorption peaks at 1494, 1380 and 1163 cm^{-1} are due to C═C, C–N stretching vibrations respectively; and the peaks at 744, 720, 735 cm^{-1} are caused by the C–H stretching vibration of either 1,10-phenanthroline or carbazole. There are sharp absorption bands at 1107, 1103, 1105 cm^{-1} for **P1**–**P3**, respectively, which should be associated with C–N vibrations at the C–N–M site [38]. With increasing the length of the polymer chain the peaks of the corresponding polymeric metal complexes show a red-shift compared with that of the free ligand. Sharp bands at 2926 and 2854 cm^{-1} are associated with the CH_2 asymmetric and symmetric stretching vibration, respectively, which illuminates that N-octylcarbazole has been successfully embedded in the molecular chain. The number average molecular weight of the coploymers (Table 1), which proved that the copolymerization has been taken place between the monomers, gives evidence of the success of the polymerization when taken together with the data of the elemental analysis of the copolymers.

Gel permeation chromatography (GPC) studies shows that **P1**–**P3** have number average molecular weight at 5.0, 4.6 and 5.4 kg/mol (4, 5 and 6 repeating units on average for **P1**–**P3**, respectively) with a relatively broad polydispersity index (PDI) between 1.81, 1.67 and 1.47 for **P1**–**P3**, respectively (shown in Table 1). As expected, **P1**–**P3** were soluble in common organic solvents such as DMF, toluene and DMSO, but present poor solubility in THF, DCM and MeOH.

Table 1
Molecular weights, thermal and optical properties of copolymers.

Polymer	P1	P2	P3
$\overline{Mn}$[a] [$\times 10^3$]	5.0	4.6	5.4
Mw/Mn	1.81	1.67	1.47
Yield (%)	49	50	45
T_g[b] [°C]	156	168	120
T_d[c] [°C]	454	489	310
$\lambda_{a,max}$[d], $\lambda_{a,onset}$	405	370,405	345,385
$\lambda_{p,max}$[e]	535	500	500
HOMO (eV)	−5.70	−5.77	−5.74
LUMO (eV)	−3.52	−3.62	−3.49
E_g^{EC}[f] (eV)	2.18	2.15	2.24

[a] Determined by gel-permeation chromatography using polystyrene as standard.
[b] Determined by DSC with a heating rate of 20 °C/min under nitrogen.
[c] The temperature at 5% weight loss under nitrogen.
[d] $\lambda_{a,max}$, $\lambda_{a,onset}$: The maxima and onset absorption from the UV–vis spectra in DMF solution.
[e] $\lambda_{p,max}$: The PL maxima in DMF solution.
[f] E_g^{EC}: Electrochemical band gap determined from cyclic voltammetry.

3.2. Optical and thermal properties of the polymers

Fig. 2 shows the absorption spectra of **DBPC** and **P1**–**P3** in DMF solution. All absorption peaks for the copolymers are shifted toward the longer-wavelength region relative to the maxima for the ligand **DBPC**. The corresponding optical data of the polymeric metal complexes are summarized in Table 1. The **DBPC** gives two distinct absorption bands, one strong absorption band in the near-UV region (280–311 nm) corresponding to the π–π* electron transitions of the conjugated molecules, and the other one in the visible region (320–402 nm) that can be attributed to an intramolecular charge transfer (ICT) between the electron acceptor metal-phenanthroline unit and the electron donating carbazole moiety [39]. In comparison with **DBPC**, the maximum absorption of **P1**–**P3** is obviously red-shifted due to the coordination of the ligand with

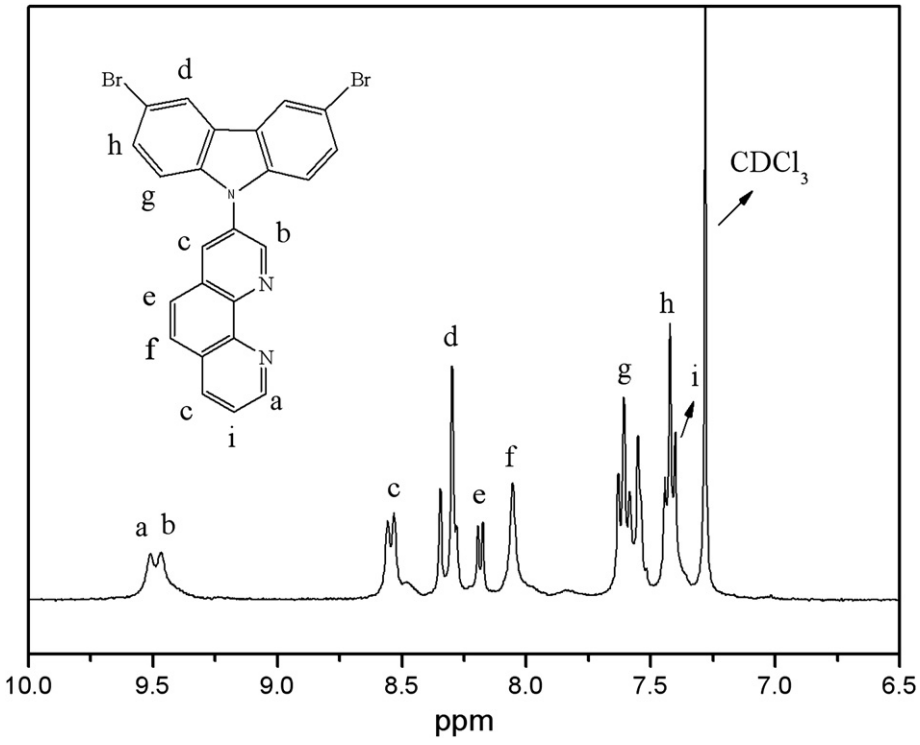

Fig. 1. ^{1}H NMR spectra of the ligand (**DBPC**) in $CDCl_3$.

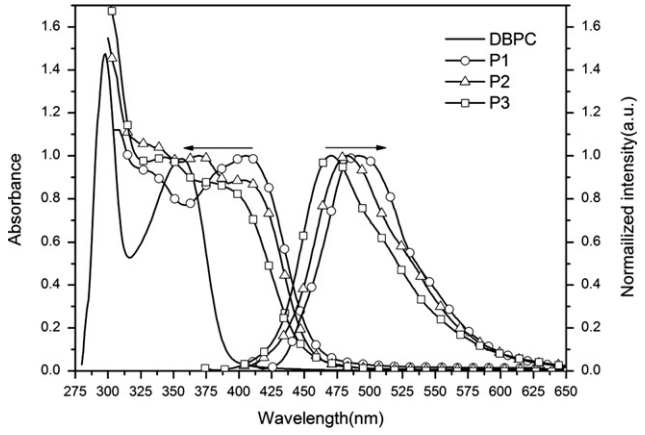

Fig. 2. Normalized absorption spectra and PL spectra of the **DBPC**, **P1**–**P3** in DMF solution.

the metal ions Zn(II), Cd(II) and Ni(II). The other weak and broad band is in the visible region (400–480 nm) that can be assigned to MLCT or d–d transition and the overlap of the π–π* transitions of the 3,6-dibromo-9-N-octyl carbazole.

Fig. 2 also shows the photoluminescence spectra of the three polymeric complexes in DMF solution. The excitation wavelengths were set to the absorption maxima from the UV–vis absorption spectra. It can be seen that the PL peak of **P1**–**P3** are at 491, 485 and 470 nm, respectively; the corresponding optical data of the polymeric metal complexes and are also summarized in Table 1.

The thermal properties of the copolymers were investigated by thermogravimetric (TGA) and differential scanning calorimetric (DSC) analyses and are also reported in Table 1. The TGA (Fig. 3) results reveal that **P1**–**P3** were thermally stable with 5% weight loss occurring at temperatures of 454 °C 489 °C and 310 °C under nitrogen, respectively, which indicate that all the polymers have excellent thermal stabilities [40]. The T_g data indicate that all the complexes possess a very high glass transition temperature, which may serve as an advantage for optoelectronic device fabrication, because the use of the materials with high transition temperatures as the dye may provide the device with greater longevity [41].

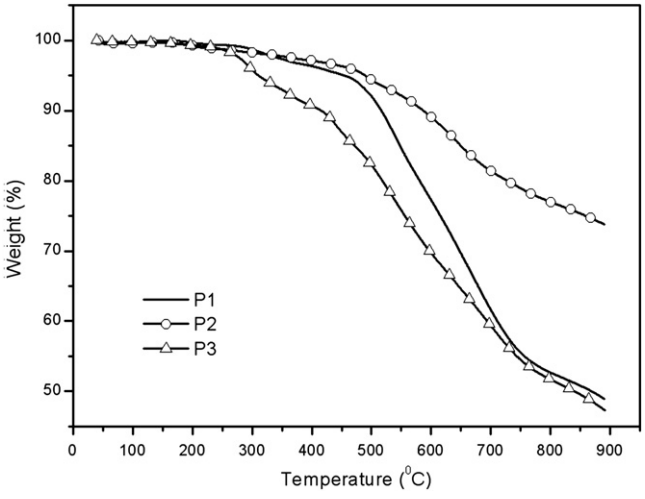

Fig. 3. TGA plots of **P1**–**P3** with a heating rate of 20 °C/min under nitrogen atmosphere.

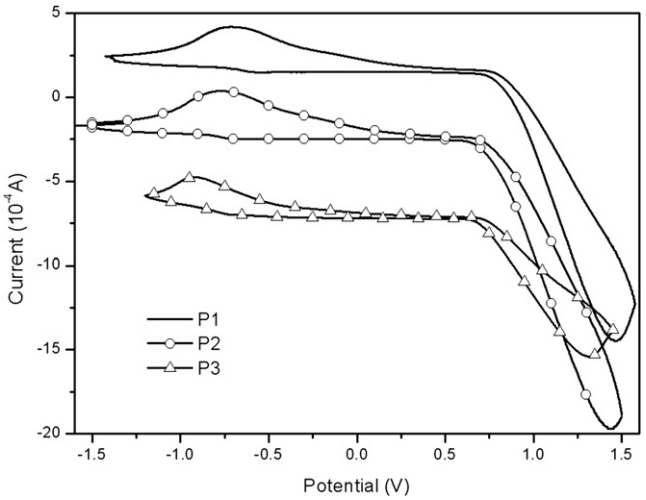

Fig. 4. CV curves of **P1**–**P3** measured in DMF solution containing $[Bu_4N]BF_6$ as supporting electrolyte at a scan rate of 100 mV/s.

3.3. Electrochemical properties

The electrochemical behavior of the obtained polymers was investigated by cyclic voltammetry, which is an important property for organic materials used in solar cells. Fig. 4 shows the cyclic voltammetry curves (CV curves) of **P1**–**P3**. The cyclic voltammetry of the complexes were measured in DMF solution containing $[Bu_4N]BF_6$ as supporting electrolyte and Ag/AgCl was used as reference electrode at a scan rate of 50 mV/s. The HOMO and LUMO are measured by cyclic voltammetry (CV). When an Ag/AgCl electrode is used as the reference electrode, the correlation can be expressed as the equation: HOMO = $-e(E_{ox} + 4.40)$ (eV); LUMO = $-e(E_{red} + 4.40)$ (eV) [42]; The corresponding data are obtained and tabulated (Table 1). The reduction and oxidation potentials of **P1** were measured to be $E_{red} = -0.88$ eV and $E_{ox} = 1.3$ eV, respectively. The energy band gap was 2.18 eV, the energy value of the HOMO was calculated to be −5.70 eV and the energy value of the LUMO was calculated to be −3.52 eV. Similarly for **P2** and **P3**, their E_g is 2.15 eV and 2.24 eV, respectively. On the basis of the CV data, the LUMO of the complexes follows the order of **P2** < **P1** < **P3,** which shows the electron accepting ability of the

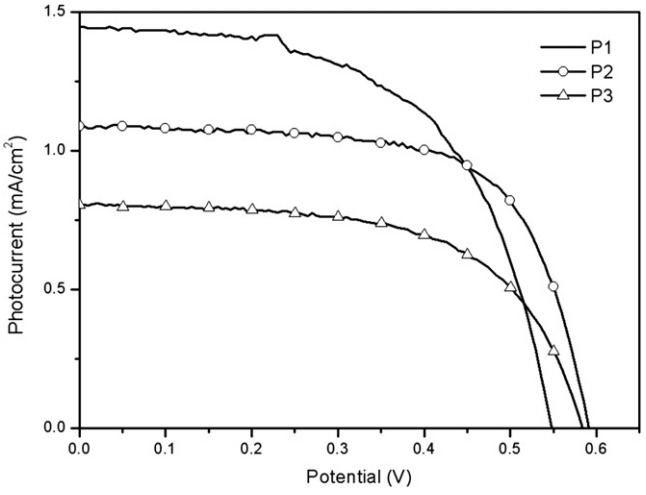

Fig. 5. *J*–*V* curves of DSSCs based on **P1**–**P3** in DMF solution.

Table 2
The data of photovoltaic performances of DSSCs.

Polymer	Solvent	Illumination time (min)	J_{sc} (mA/cm^2)	V_{oc} (V)	ff (%)	η (%)
P1	DMF	8	1.088	0.59	64.8	0.42
P2	DMF	8	1.45	0.55	55	0.44
P3	DMF	6	0.805	0.58	59.3	0.29

complexes following the order of **P2** > **P1** > **P3** [43]. E_g of the complexes follows the order of **P2** < **P1** < **P3,** so **P2** is more suitable for the fabrication of optoelectronic devices than either **P1** or **P3**, because a relatively low E_g can absorb light efficiently which is very important to improve power conversion efficiencies [44].

3.4. Photocurrent-voltage measurements

Fig. 5 shows the current density–voltage (J–V) curves of DSSCs devices based on the three polymeric metal complexes **P1**–**P3**. The corresponding open-circuit voltage (V_{oc}), short-circuit current density (J_{sc}), fill factor (ff) and power conversion efficiency (η) are listed in Table 2. It can be seen that the V_{oc} values of **P1**–**P3** dyes are 0.59 V, 0.55 V and 0.58 V, respectively and the corresponding ff values are 0.648, 0.55 and 0.593. However, the J_{sc} values increased from 0.805 mA/cm^2 for **P3** to 1.088 mA/cm^2 for **P1** and 1.45 mA/cm^2 for **P2**. The power conversion efficiency based on **P3** reached 0.29%, which is lower than that of the device based on **P1** (0.42%) and **P2** (0.44%). The result could be due to the significant difference between d^{10} Zn(II), Cd(II) complexes and low spin d^8 Ni(II) complexes. The d^{10} metal complexes possessed higher kinetic stability to d^8 metal complexes. The low J_{sc} is ascribed to the weak adsorption onto the surface of TiO_2, low charge separation and low transportation efficiency. However, these initial results are not comparable with state of the art ruthenium dyes such as N719, and further work on optimizing the device performance is under investigation.

4. Conclusions

In summary, we report the synthesis and characterization of three novel copolymers containing 1,10-phenanthroline Zn(II), Cd(II) and Ni(II) complexes with carbazole units. The three materials have good stability and they also exhibit good open-circuit voltages, fill factors but moderate power conversion. The power conversion efficiencies of **P1**–**P3** fill 0.42%, 0.44% and 0.29%, respectively, suggesting further optimization is essential before application in DSSCs.

However, in order to obtain outstanding η, there are still many challenges to surmount. First of all, J_{sc} based on all the materials is very low, due to the low adsorption affinities on the TiO_2. So, one or two anchoring groups such as –COOH or $-SO_3H$ groups should be introduced in the structure [45]. Further structural optimization with broad spectral coverage and excellent charge separation and transportation are expected to produce more efficient photosensitizers. Our works toward these directions are underway.

References

[1] Seo KD, Song HM, Lee MJ, Pastore M, Anselmi C, Angelis FD, et al. Coumarin dyes containing low-band-gap chromophores for dye-sensitised solar cells. Dyes Pigm 2011;90:304–10.
[2] Grätzel M. Solar energy conversion by dye-sensitized photovoltaic cells. Inorg Chem 2005;44:6841–51.
[3] Chiba Y, Islam A, Watanabe Y, Komiya R, Koide N, Han L. Dye-sensitized solar cells with conversion efficiency of 11.1%. Jpn J Appl Phys 2006;45:638–40.
[4] Gao F, Wang Y, Shi D, Zhang J, Wang M, Jing X, et al. A new heteroleptic ruthenium sensitizer enhances the absorptivity of mesoporous titania film for a high efficiency dye-sensitized solar cell. J Am Chem Soc 2008;23:2635–7.
[5] Hagfeldt A, Boschloo G, Sun LC, Kloo L, Pettersson H. Dye-sensitized solar cells. Chem Rev 2010;10:6595–663.
[6] Mishra A, Fischer MKR, Bäuerle P. Metal-free organic dyes for dye-sensitized solar cells: from structure property relationships to design rules. Angew Chem Int Ed 2009;48:2474–99.
[7] Ito S, Miura H, Uchida S, Takata M, Sumioka K, Liska P, et al. High-conversion-efficiency organic dye-sensitized solar cells with a novel indoline dye. Chem Commun; 2008:5194–6.
[8] Nogueira AF, Longo C, De Paoli M-A. Polymers in dye sensitized solar cells: overview and perspectives. Coord Chem Rev 2004;248:1455–68.
[9] Xu MF, Wenger S, Bala H, Shi D, Li RZ, Zhou YZ, et al. Tuning the energy level of organic sensitizers for high-performance dye-sensitized solar cells. J Phys Chem C 2009;113:2966–73.
[10] Zhen FZ, Eshbaugh AA, Schanze KS. Low-Bandgap donor-acceptor conjugated polymer sensitizers for dye-sensitized solar cells. J Am Chem Soc 2011;133:3063–9.
[11] Chindaduang A, Duangkaew P, Pratontep S, Tumcharern G. Composite polymer electrolyte for dye-sensitized solar cells: role of multi-walled carbon nanotubes. Adv Mater Res 2010;31:93–4.
[12] Liu XZ, Zhang W, Uchida S, Cai LP, Liu B, Ramakrishna S. An efficient organic-dye-sensitized solar cell with in situ polymerized poly(3,4-ethylene dioxythiophene) as a hole-transporting material. Adv Mater 2010;22:150–5.
[13] Zou Y, Gendron D, Aïch RB, Najari A, Tao Y, Leclerc M. A high-mobility low-bandgap poly(2,7-carbazole) derivative for photovoltaic applications. Macromolecules 2009;42:2891–4.
[14] Patra D, Sahu D, Padhy H, Kekuda D, Chu CW, Lin HC. Synthesis and applications of 2,7-carbazole-based conjugated main-chain copolymers containing electron deficient bithiazole units for organic solar cells. J Polym Sci Part A Polym Chem 2010;48:5479–89.
[15] Tieke B, Rabindranath AR, Zhang K, Zhu Y. Conjugated polymers containing diketopyrrol-opyrrole units in the main chain. Beilstein J Org Chem 2010;6:830–45.
[16] Horiuchi T, Miura H, Uchida S. Highly-efficient metal-free organic dyes for dye-sensitized solar cells. Chem Commun; 2003:3036–7.
[17] Zhang X, Steckler TT, Dasari RR, Ohira S, Potscavage WJ, Tiwari SP, et al. Dithienopyrrole-based donor-acceptor copolymers: low band-gap materials for charge transport, photovoltaics and electrochromism. J Mater Chem 2010;20:123–34.
[18] Huo L, Chen HY, Hou J, Chen TL, Yang Y. Low band gap dithieno[3,2-b:2′,3′-d]silole-containing polymers, synthesis, characterization and photovoltaic application. Chem Commun; 2009:5570–2.
[19] Fan HJ, Zhang ZG, Li YF, Zhan XW. Copolymers of fluorene and thiophene with conjugated side chain for polymer solar cells: effect of pendant acceptors. J Polym Sci Part A Polym Chem 2011;49:1462–70.
[20] Chen MH, Hou J, Hong Z, Yang G, Sista S, Chen LM, et al. Efficient polymer solar cells with thin active layers based on alternating polyfluorene copolymer/fullerene bulk heterojunctions. Adv Mater 2009;21:4238–42.
[21] Zhang WW, Mao WL, Hu YX, Tian ZQ, Wang ZL, Meng QJ. Phenothiazine-anthraquinone donor-acceptor molecules: synthesis, electronic properties and DFT-TDDFT computational study. J Phys Chem A 2009;113:9997–10004.
[22] Huang JH, Ho ZY, Kekuda D, Chang Y, Chu CW, Ho KC. Effects of nano-morphological changes on the performance of solar cells with blends of poly[9,9-dioctyl-fluoreneco-bithiophene] and a soluble fullerene. Nanotechnology 2009;20. 025202.
[23] Raj V, Madheswari D, Ali MM. Chemical formation, characterization and properties of polycarbazole. J Appl Polym Sci 2010;116:147–54.
[24] Han F, Chi L, Liang X, Ji S, Liu S, Zhou F, et al. 3,6-Disubstituted carbazole-based bisboronic acids with unusual fluorescence transduction as enantioselective fluorescent chemosensors for tartaric acid. J Org Chem 2009;74:1333–6.
[25] Bloudin N, Leclerc M. Poly(2,7-carbazole)s: structure-property relationships. Acc Chem Res 2008;41:1110–9.
[26] Watanabe M, Nishiyama M, Yamamoto T, Koie Y. Palladium/P(*t*-Bu)$_3$-catalyzed synthesis of *N*-aryl azoles and application to the synthesis of 4,4′,4″-tris(*N*-azolyl) triphenylamines. Tetrahedron Lett 2000;41:481–3.
[27] Kim D, Lee JK, Kang SO, Ko J. Molecular engineering of organic dyes containing N-aryl carbazole moiety for solar cell. Tetrahedron 2007;63:1913–22.
[28] McMillin DR, Buckner MT, Ahn BT. A light-induced redox reaction of bis(2,9-dimethyl-l,10-phenanthroline)copper(I). Inorg Chem 1977;16:943–5.
[29] McMillin DR, McNett KM. Photoprocesses of copper complexes that bind to DNA. Chem Rev 1998;98:1201–19.
[30] Meyer M, Albrecht-Gary AM, Dietrich-Buchecker CO, Sauvage JP. π–π Stacking-induced cooperativity in copper(I) complexes with phenanthroline ligands. Inorg Chem 1999;38:2279–87.
[31] Armaroli N. Photoactive Cu(I)-phenathrolines. A viable alternative to Ru(II)-polypyridines. Chem Soc Rev 2001;30:113–24.
[32] Tzalis D, Tor Y, Failla S, Siegel JS. Simple one-step synthesis of 3-bromo- and 3,8-dibromo-1,10-phenanthroline: fundamental building blocks in the design of metal chelates. Tetrahedron Lett 1995;36:3489–90.
[33] Hameurlaine A, Dehaen W, Peng H, Xie Z, Tang BZ. Synthesis and light-emitting properties of a new conjugated polymer containing carbazole and quinoxaline moieties. J Macromol Sci Part A Pure Appl Chem 2004;41:295–303.

[34] Kanelidis I, Elsner V, Bötzer M, Butz M, Lesnyak V, Eychmüller A, et al. Synthesis and characterization of aminofunctional, blue light-emitting copolymers and their composites with CdTe nanocrystals. Polymer 2010;51:5669–73.
[35] Zhu Y, Rabindranath AR, Beyerlien T, Tieke B. Highly luminescent 1,4-Diketo-3,6-diphenylpyrrolo[3,4-c]pyrrole-(DPP-) based conjugated polymers prepared upon Suzuki coupling. Macromoleculars 2007;40:6983–9.
[36] Ullmann F, Bielecki J. Ueber Synthesen in der Biphenylreihe. Chem Ber 1901;34:2174–8.
[37] Yamamoto T, Yamada W, Takagi M, Kizu K, Maruyama T, Ooba N, et al. π-Conjugated soluble poly(aryleneethynylene) type polymers, preparation by palladium-catalyzed coupling reaction, nonlinear optical properties, doping, and chemical reactivity. Macromolecules 1994;27:6620–6.
[38] Hall D, Rae AD, Waters TN. The crystal structures of the chloroform solvate of dioxodi-8-quinolinolato-8-quinolinoluranium(VI). Acta Cryst 1967;22:258–68.
[39] McClenaghan ND, Passalacqua R, Loiseau F, Campagna S, Verheyde B, Hameurlaine A, et al. Ruthenium (II) dendrimers containing carbazole-based chromophores as branches. J Am Chem Soc 2003;125:5356–65.
[40] Ng S, Xu JM, Chan HSO. Thermal stability and kinetic study of conductive polymers containing phenylene and bithiophene units. Synth Met 2000;110:31–6.
[41] Tokito S, Tanaka H, Noda K, Okada A, Taga Y. Thermal stability in oligomeric triphenylamine/tris(8-quinolinolato) aluminum electroluminescent devices. Appl Phys Lett 1997;70:1929–31.
[42] Nazeerudin MK, Kay A, Rodicio I, Humphry-Bake R, Müller E, Liska P, et al. Conversion of light to electricity by cis-X2bis(2,2′-bipyridyl-4,4′-dicarboxylate) ruthenium(II) charge-transfer sensitizers (X = Cl-, Br-, I-, CN-, and SCN-) on nanocrystalline titanium dioxide electrodes. J Am Chem Soc 1993;115:6382–90.
[43] Sun Y, Wang S. Conjugated triarylboryl donor acceptor systems supported by 2,2′-bipyridine: metal chelation impact on intraligand charger transfer emission, electron accepting ability, and “Turn-on” fluoride sensing. Inorg Chem 2009;48:3755–67.
[44] Cheng YJ, Yang SH, Hsu CS. Synthesis of conjugated polymers for organic solar cell applications. Chem Rev 2009;109:5868–923.
[45] Wang ZS, Li FY, Huang CH. Photocurrent enhancement of hemicyanine dyes containing RSO_3 group through treating TiO_2 films with hydrochloric acid. J Phys Chem B 2001;105:9210–7.